

Permeability of illite-bearing shale: 2. Influence of fluid chemistry on flow and functionally connected pores

Ohmyoung Kwon,¹ Bruce E. Herbert, and Andreas K. Kronenberg

Department of Geology and Geophysics, Texas A&M University, College Station, Texas, USA

Received 27 February 2004; revised 9 June 2004; accepted 14 July 2004; published 14 October 2004.

[1] Bedding-parallel permeability of illite-rich shale of the Wilcox formation has been investigated using distilled water and 1 M solutions of NaCl, KCl, and CaCl₂ as pore fluids. Despite low modal concentrations of swelling clays, specimens expand upon fluid saturation and permeabilities depend on fluid composition. Permeabilities to flow of 1 M CaCl₂ are 3–5 times greater than values measured for the other pore fluids, suggesting sensitivity to exchange of divalent cations for monovalent cations at clay mineral surfaces. Permeabilities of individual samples exhibit nonrecoverable changes with sequential changes in composition of incoming fluid. Permeabilities k at varying effective pressure P_e fit a cubic law $k = k_0 [1 - (P_e/P_1)^m]^3$, where m and P_1 are independent of fluid composition, and k_0 is greater for transport of 1 M CaCl₂ than that for transport of the other pore fluids. Assuming that fluid conduits have crack-like dimensions, the lack of sensitivity of m and P_1 to fluid composition suggests that surface roughness and asperity stiffness of conduits are unaffected by cation exchange, while changes in k_0 reflect changes in the clay-fluid interfaces of the connected pore space.

INDEX TERMS: 5114 Physical Properties of Rocks: Permeability and porosity; 5139 Physical Properties of Rocks: Transport properties; 1832 Hydrology: Groundwater transport; 3947 Mineral Physics: Surfaces and interfaces; 1045 Geochemistry: Low-temperature geochemistry; **KEYWORDS:** permeability, shale, fluid chemistry

Citation: Kwon, O., B. E. Herbert, and A. K. Kronenberg (2004), Permeability of illite-bearing shale: 2. Influence of fluid chemistry on flow and functionally connected pores, *J. Geophys. Res.*, 109, B10206, doi:10.1029/2004JB003055.

1. Introduction

[2] Abnormal pore pressures in sedimentary basins are commonly associated with occurrences of shales [Dickinson, 1953; Dickey et al., 1968; Magara, 1971; Chapman, 1972, 1982, 1994; Schmidt, 1973; Berg and Habeck, 1982; Freed and Peacor, 1989; Bigelow, 1994]. Elevated pore pressures may be generated by a number of processes, including compaction of fluid-saturated sediments [Dickinson, 1953; Magara, 1975a; Hart et al., 1995; Smith and Wiltschko, 1996], transformation of smectites to illite [Powers, 1967; Burst, 1969; Freed and Peacor, 1989], thermal expansion of fluids [Barker, 1972; Magara, 1975b; Sharp, 1983], and the formation of oil and gas from organic constituents of shales [Hedberg, 1974; Meissner, 1978; Momper, 1978; Illing, 1938; Barker, 1987, 1990; Spencer, 1987, 1994]. Once generated, abnormal pressures may dissipate to equilibrium values along the hydrostatic pressure gradient unless upward fluid flow is limited by overlying units of high capillarity or intrinsically low permeability. Given that abnormal pressures are associated with hydrocarbon gener-

ation, shales may form seals to upward migration because of their high capillary pressures to nonwetting fluids [e.g., Berg, 1975; Vavra et al., 1992; Schlomer and Krooss, 1997; Hao et al., 2000]. Shales may also limit the flow of aqueous pore fluids if their permeabilities are sufficiently low [Bredehoeft and Hanshaw, 1968; Bradley, 1975; Hunt, 1990; Deming, 1994].

[3] Shale permeabilities vary widely (from 10^{-16} m² to 10^{-23} m²) with values well above and below those required for pressure seals over characteristic geologic and reservoir production times [Young et al., 1964; Magara, 1971; Lin, 1978; Bredehoeft et al., 1983; Katsube et al., 1991; Dewhurst et al., 1998, 1999; Kwon et al., 2001]. Permeabilities of shales depend on porosity, clay mineralogy and content, and texture [Katsube et al., 1991; Schlomer and Krooss, 1997; Dewhurst et al., 1998, 1999; Revil and Cathles, 1999; Kwon et al., 2004], all of which may change with burial [e.g., Hower et al., 1976; Lee et al., 1985; Addis and Jones, 1985; Dzevanishir et al., 1986; Kim et al., 1999].

[4] Permeabilities may also depend on pore fluid composition if pore throats available for fluid flow are modified by local clay swelling and formation of hydrated complexes at clay-fluid interfaces [Scott and Smith, 1966; Norrish, 1973; Van Olphen, 1977; Sparks, 1995; Spósito et al., 1999]. Clay aggregates made up of swelling clays exhibit extremely low permeabilities to the flow of water [Moore et

¹Now at Core Laboratories, Petroleum Services, Houston, Texas, USA.

al., 1982; Faulkner and Rutter, 2000]. Hydration and expansion of swelling clays may be affected by changing fluid composition, as interlayer cations are replaced by solutes of the pore fluid. Correspondingly, permeabilities of clay aggregates depend on electrolytes in the pore fluid [Whitworth and Fritz, 1994; Mesri and Olson, 1971; Olsen, 1972]. Permeabilities of deeply buried shales, with abundant illite and little or no smectites, are expected to show less chemical sensitivity than permeabilities of shallow mudstones with higher modal swelling clay contents. Yet, transport properties may continue to depend on fluid composition if cation exchange occurs at intergranular clay-fluid interfaces, and pores are affected by changing dimensions of the diffuse double layer.

[5] Compositions of pore fluids within sedimentary rocks vary considerably according to their origin, modification through reaction with sediments (particularly with clay minerals), patterns of advection, and thermal history [e.g., Siever et al., 1965; Fournier and Truesdell, 1973; Magara, 1974; Morse and Mackenzie, 1990; Harrison and Summa, 1991; Longstaffe et al., 1992; Bjorlykke and Gran, 1994; Hanor, 1994]. Interstitial pore fluids of sediments of the northern Gulf Coast, for example, consist of brines that vary spatially within individual units, with salt contents of fluids in Tertiary sediments of Louisiana [Timm and Maricelli, 1953; Chilingarian et al., 1994] reaching 4.5 times the salinity of standard mean ocean water (SMOW, 35,000 ppm). Major cations of pore fluids of the Gulf Tertiary section include Na, K, Ca, and Mg [Kharaka et al., 1977; Morton and Land, 1987; Land and Macpherson, 1992; Hanor, 1994; Land, 1995]. In analyses of sidewall core samples from shale sections in the Manchester field, Calcasieu Parish, Louisiana, Schmidt [1973] found that Na was the major cation of interstitial aqueous fluids with lower concentrations of K, Ca, and Mg. Surface complexes of clay minerals in shales may thus involve both monovalent and divalent cations with potential consequences for the dimensions of critical pore throats, electrical character of fluid-clay interfaces, and the functionally connected porosity.

[6] In this paper, we report on laboratory measurements of permeability for low-porosity, illite-rich shale specimens of the Wilcox formation and observed effects of fluid composition on transport properties. Permeabilities to distilled water and 1 *M* (molar) solutions of NaCl, KCl, and CaCl₂ are reported for transport parallel to bedding for samples saturated over extended times with fluid of a given composition, as well as samples subjected to sequential changes in incoming fluid composition. The sources of chemical effects on fluid transport and connected pore space are constrained by accompanying bulk expansion measurements of samples saturated with the same pore fluids as used in the permeability measurements and X-ray diffraction measurements of clay interlayer dimensions. Permeability across bedding of Wilcox shale and effects of clay content and loading on permeability are addressed by Kwon et al. [2004] for 1 *M* NaCl pore fluid.

2. Experimental Methods

2.1. Specimen Selection and Preparation

[7] Wilcox shale specimens were prepared from the same core as used in the accompanying paper [Kwon et al., 2004],

selecting horizons of relatively low clay content (40–50%) from core taken at depths of 3955–3956 m (12,975–12,979 feet). On the basis of X-ray diffraction of dehydrated and glycerated powder samples [Ibanez and Kronenberg, 1993], illite is the predominant clay mineral (29%) of this shale, with lesser quantities of chlorite (14%), kaolinite (10%), and only a trace of mixed layer illite-smectite (~2%); the remainder of the shale consists of quartz (37%) and lesser quantities of pyrite, calcite, feldspar, and organics (8% combined). Connected porosities determined on the basis of weight gain following immersion in 1 *M* NaCl solution (using a density of 1040 kg/m³) [Wolf et al., 1979] range from 7 to 8%. Permeabilities measured parallel to bedding are higher than measured perpendicular to bedding and microstructural observations suggest that flow parallel to bedding is enhanced by crack-like bedding-parallel voids within and adjacent to oriented clays and clay layers [Kwon et al., 2004]. No special procedures were followed to preserve the original pore fluid content of the shale; thus some modification of clays and their surface hydration may have occurred before we acquired the core.

[8] Oriented rectangular samples were prepared for bulk expansion measurements of swelling upon exposure to the same fluids as used in the permeability experiments. Orthogonal faces were cut parallel and perpendicular to bedding with a diamond wafer saw and surfaces ground square; final dimensions measured ~5 mm normal to bedding and 4 mm × 8.5 mm in the bedding plane. Samples for powder X-ray diffraction measurements were prepared by mechanical grinding, mounting powders on glass plates either dry or in fluid. Right cylindrical specimens (25.4 mm in length and 12.5 mm in diameter) were prepared for permeability measurements by diamond coring parallel to bedding and grinding ends parallel to each other and perpendicular to their cylindrical axes.

[9] As permeabilities vary considerably among samples of Wilcox shale due to variations in clay content and microstructure [Kwon et al., 2004], samples for this study were selected from individual horizons with nearly identical lithologies. Geometrical constraints and the shale core diameter (3.5 inches) limited us to just three specimens for permeability measurements from any one horizon. Three specimens were selected from a single horizon designated 76A and permeabilities measured using distilled water and 1 *M* solutions of NaCl and KCl. Three specimens were taken from another horizon 76B, just 20 mm above horizon 76A and permeabilities measured using 1 *M* NaCl and 1 *M* CaCl₂. Additional specimens for permeability tests with sequential changes in composition of the incoming fluid were taken from horizons 76C and 76D, which were 0.20 and 0.50 m, respectively, above horizon 76A.

2.2. Specimen Saturation and Expansion Measurement

[10] Upon acquisition of the core, the shale used in this study had a water content of 2.1% (based on weight loss upon heating to 210°C), with much of the open pore space (8%) free of the original pore fluid. Specimens selected for expansion and permeability measurements were immersed and their pore space saturated, either by distilled water or 1 *M* solutions of NaCl, KCl, or CaCl₂. The 1 *M* brine solutions were prepared by dissolving weighed quantities of reagent grade salts in distilled water. Fluids of each com-

position were introduced into specimen pores using multiple vacuum impregnation procedures. Samples were immersed in fluid within a vacuum chamber and air within pores removed by sequentially applying a vacuum to the immersed sample for 30 min and bleeding atmospheric pressure back into the chamber. Upon initial application of vacuum, bubbles were vigorously expelled from the sample and fluid. This sequential application of vacuum and bleeding was repeated >10 times (over 2–3 days) until bubbles ceased to emerge from the sample. Rectangular specimens for bulk expansion measurements remained in fluid for an extended time (>3 weeks) before their dimensions were remeasured, changing the solutions occasionally to maintain constant composition and subjecting the samples to another cycle of vacuum impregnation. Cylindrical specimens for permeability measurements were stored, immersed in fluid of the desired composition until their jackets were sealed to end closures, pressurized, and pore pressure equilibrium achieved.

[11] During immersion, fluids had access to all six sides of the rectangular specimens used to measure bulk expansion while they had access to only the ends of cylindrical specimens used in permeability measurements. Prior to immersion, specimens for permeability tests were placed in heat shrinkable polyolefin jackets with a thin coat of RTV silicone applied to their cylindrical walls to form a seal between the specimen and jacket. Saturation of cylindrical specimens used in permeability tests was assured by later pressure injection procedures as specimens were subjected to increased confining and pore pressures. These specimens were sealed to end closures with pore pressure ports at both ends, inserting a layer of glass fiber felt (Fiberfrax, Carborundum Corp.) at each end to provide uniform fluid access. The seal between the end closures and jacket was accomplished by way of Nichrome wires, tied over grooves machined in each closure.

[12] Once specimens used in the permeability measurements were sealed, they were placed in the pressure vessel of an apparatus (LSR, J. Handin Rock Deformation Laboratory) capable of applying a confining pressure to the jacketed specimen walls and imposing a gradient in pore fluid pressure across the specimen. The portion of the pore pressure system that required disassembly between experiments was placed under a vacuum for 30 min (to remove trapped air) and then filled with either distilled water or one of the 1 M brine solutions. Specimens were first subjected to a confining pressure P_c of 3 MPa, and then to an internal fluid pressure P_f of 2 MPa. Fluid in contact with both specimen ends was pressurized, holding P_c constant, and bled repeatedly to ensure complete filling of the pore pressure system by the fluid. Samples were judged to be saturated by a marked increase in sensitivity of P_f to confining pressure P_c perturbations [Green and Wang, 1986]. Once P_f remained constant over 4–5 hours, it was considered at equilibrium with the internal pore pressure P_p of the sample. The amount of pore fluid added to samples by increasing fluid pressure was small compared with quantities previously added by vacuum impregnation (<3% of that added by vacuum treatment).

[13] The dimensions of rectangular specimens (x and y in the bedding plane and z normal to bedding) were measured before and after saturation using a micrometer with a

resolution of ± 0.004 mm. Length changes and volumetric expansions were determined, averaging results for five specimens saturated by distilled water, 10 specimens saturated by 1 M NaCl, five specimens saturated by 1 M KCl, and 10 specimens saturated by 1 M CaCl₂. Swelling of the clay minerals was tested by X-ray diffraction of powder samples immersed in the same fluids as used in the bulk expansion and permeability tests, measuring peak heights and widths (at their half height intensities) of basal clay mineral diffractions. Peak intensities at d spacings of 14.2 Å (chlorite and potentially a swelling clay) and 7.1 Å (predominantly kaolinite) were compared, normalizing by the peak intensity at 9.9 Å (of nonswelling illite).

2.3. Permeability Measurements

[14] Permeabilities for flow of distilled water and 1 M solutions of NaCl, KCl, and CaCl₂ were measured parallel to bedding by the same transient pulse method as used in the accompanying paper on Wilcox shale flow properties [Kwon *et al.*, 2004]. Confining and pore pressures were increased from $P_c = 3$ MPa and $P_p = 2$ MPa to the desired experimental conditions ($P_c = 13, 15, 18$ MPa, $P_p = 10$ MPa) in a slow, stepwise manner (to permit internal pore pressure P_p to keep up with the applied fluid pressure P_f of the pore pressure system). Throughout this pressurization procedure, the difference in pressures ($P_c - P_p$) was not permitted to exceed the effective pressure ($P_e = 3, 5, 8$ MPa) at which permeability was to be measured. Permeabilities for individual specimens saturated by pore fluid of a given composition were determined by imposing a step in fluid pressure at one specimen end (increasing P_f by $\leq 15\%$ of the initial P_p) and measuring the decay in fluid pressure difference ($P_{up} - P_{dn}$) associated with flow along the length of the cylindrical specimen, where P_{up} is the higher, upstream fluid pressure and P_{dn} is the lower, downstream fluid pressure [Brace *et al.*, 1968; Sutherland and Cave, 1980; Trimmer, 1981; Kwon *et al.*, 2004]. In all reported experiments, the difference in fluid pressure across the specimen followed the expression

$$(P_{up} - P_{dn}) = \Delta P_i e^{-\theta t} \quad (1a)$$

within experimental error, where ΔP_i is the initial fluid pressure difference at time $t = 0$, and the decay constant θ is given by

$$\theta = (kA/\eta\beta L)(1/V_{up} + 1/V_{dn}), \quad (1b)$$

where permeability k can be calculated for known values of the specimen cross-sectional area A and length L , the fluid's dynamic viscosity η and compressibility β , and the volumes V_{up} and V_{dn} , respectively, of the upstream and downstream portions of the pore pressure system. Fluid viscosities used in the analysis come from values tabulated by Wolf *et al.* [1979]; $\eta = 0.99 \times 10^{-9}$ MPa·s for distilled water and $\eta = 1.1 \times 10^{-9}$ MPa s, 0.99×10^{-9} MPa s, and 1.36×10^{-9} MPa s for 1 M solutions of NaCl, KCl, and CaCl₂, respectively. Because of uncertainties in compressibilities of the 1 M KCl and CaCl₂ solutions at experimental conditions, we used a single value of β for all the fluids used, equivalent to that of distilled water (4.56×10^{-4} MPa⁻¹, taken from ASME steam tables) [Meyer *et al.*,

Table 1. Expansion of Wilcox Shale Upon Saturation

Fluid	Length Changes in Percent Elongation		
	Parallel to Bedding (x)	Parallel to Bedding (y)	Perpendicular to Bedding (z)
H ₂ O, distilled	0.33	0.32	0.90
1 M NaCl	0.33	0.30	0.97
1 M KCl	0.16	0.14	0.47
1 M CaCl ₂	0.45	0.44	1.29

1979]. Volumes of upstream and downstream reservoirs of the fluid pressure system ($V_{up} = 15.1$ mL, $V_{dn} = 24.4$ mL) were determined from their effective compressibilities, isolating each reservoir, and imposing steps in pressure much like those in the permeability experiments.

[15] Instrumental errors in fluid pressure measurements (± 0.02 MPa) and our ability to determine θ over the decay times of the tests led to an uncertainty in permeability k of only 1–3%. However, tests of reproducibility, measuring permeability for the same sample at the same effective pressure, indicate an uncertainty in k of 10% and samples taken from different lithologic horizons may show much greater variation ($\pm 70\%$) associated with real differences in lithology, pore structure, and the inelastic response of pore space to P_e . Permeabilities to pore fluids of different compositions were thus compared only for specimens taken from the same horizon. Errors in absolute k values could be introduced by errors in our upstream and downstream reservoir volume determinations or any departures in fluid viscosity η or compressibility β from the values we used. On the basis of compressibilities reported for distilled water and 1 M NaCl [Lide, 1997], real differences in β for the different fluids could lead to errors in permeability of $\sim 10\%$. Confining pressures P_c during the transient pulse measurements of k were controlled to within ± 0.2 MPa and measured within ± 0.06 MPa, leading to an uncertainty in reported values of ($P_c - P_p$) of ± 0.07 MPa just before the upstream fluid pressure P_{up} was increased to impose a fluid pressure gradient. Once the upstream pressure P_{up} was increased, true effective pressures within the specimen varied spatially as well as temporally. For consistency, we report $P_e = (P_c - P_p)$ just before any pore pressure gradients were imposed; any offset in k associated with P_e variations should not affect relative comparisons of k , at a given set of P_c , P_p conditions, for fluids of different compositions.

[16] The sensitivity of permeability k to effective pressure P_e was tested by applying sequentially higher confining pressures to individual specimens, so as to eliminate sample-to-sample variations, while maintaining a constant pore pressure. Much as found earlier for 1 M NaCl in Wilcox shale [Kwon *et al.*, 2001, 2004], permeability k varies with P_e by a cubic law of the form

$$k = k_0[1 - (P_e/P_1)^m]^3, \quad (2)$$

where k_0 is a reference state permeability (at $P_e = 0$) and parameters m and P_1 describe the geometry and properties of the conductive pore space [Gangi, 1978]. Parameters k_0 , m , and P_1 were determined by iterative forward modeling and compared for different pore fluids using results of samples taken from the same lithologic horizon.

[17] Despite our strategy to isolate variations in permeability due to sample lithology and pore structure from those due to fluid composition and fluid-mineral interactions, variations of $\pm 10\%$ indicate that lithologic variations in Wilcox shale occur even within the same horizon. We therefore performed an additional series of permeability experiments using individual samples and measuring k following sequential changes in incoming pore fluid composition (all at the same $P_e = 3$ MPa, $P_p = 10$ MPa). Two sets of fluid exchange experiments were conducted on individual specimens. The first set of experiments was conducted changing pore fluids from distilled water, to a 1 M NaCl solution, and then back to distilled water. The second set was conducted changing pore fluids from a 1 M NaCl solution, to a 1 M CaCl₂ solution, and then to a 1 M NaCl solution.

[18] Between each permeability measurement of these experiments, the sample was carefully removed from the apparatus, immersed in the new fluid, and subjected to vacuum impregnation procedures for 3 days, changing the solution several times to maintain a nearly constant fluid composition during ion exchange with the specimen. Once the sample was placed back into the apparatus, the pore pressure system was filled with the new fluid and P_c was increased to 3 MPa. Two equivalent pore volumes of fluid were flushed through the specimen by increasing the fluid pressure in the downstream reservoir to 2.5 MPa while the upstream reservoir was left open to atmosphere. After the pore fluid was flushed through the sample, fluid in the upstream reservoir was replaced by fluid of the new composition. After this procedure, P_c and P_p were stepwise raised as before to the same conditions ($P_c = 13$ MPa, $P_p = 10$ MPa) and permeability remeasured. While sample-to-sample variations in pore structure were eliminated in these experiments, we encountered permanent changes in permeability with sequential changes in fluid composition that we attribute to nonrecoverable cation exchange at clay-fluid interfaces.

3. Experimental Results

[19] Wilcox shale expansion and powder X-ray diffraction results are listed in Tables 1 and 2, respectively, and are illustrated in Figures 1 and 2 for samples immersed in distilled water and 1 M solutions of NaCl, KCl, and CaCl₂. Increases in dimension of rectangular samples upon fluid saturation are tabulated (in % elongation) in two orthogonal directions (x and y) within bedding and one (z) perpendicular to bedding. X-ray peak heights of 14.2 Å and 7.1 Å diffractions are listed, normalized by the 9.9 Å peak height,

Table 2. Powder X-Ray Diffraction of Wilcox Shale

Coexisting Fluid	Relative Peak Intensity ^a		Peak Width, ^b deg		
	14.2 Å	7.1 Å	14.2 Å	9.9 Å	7.1 Å
H ₂ O, distilled	0.20	0.85	0.30	0.22	0.33
1 M NaCl	0.25	1.35	0.15	0.22	0.33
1 M KCl	0.20	1.05	0.35	0.21	0.33
1 M CaCl ₂	0.20	0.95	0.20	0.20	0.34

^aNormalized by peak intensity measured at $2\theta = 8.84^\circ$ due to 9.9 Å Illite basal diffraction.

^bWidth of diffraction determined at half the peak height.

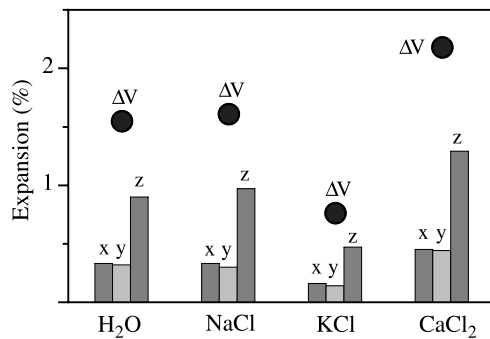


Figure 1. Dimensional expansion results for Wilcox shale specimens immersed in distilled water, 1 M NaCl, 1 M KCl, and 1 M CaCl₂ and measured in orthogonal directions *x* and *y* within bedding and in the direction *z* perpendicular to bedding. Volumetric strains, obtained by summing the three orthogonal strain determinations, are shown as dots and labeled ΔV .

and widths of diffractions represent widths measured at half the peak height. Permeabilities measured parallel to bedding are organized in Tables 3 and 4 by sampling horizon (e.g., horizon 76A), specimen number (e.g., WS22.6) and measurement sequence (e.g., WS22.6-1, WS22.6-2, and WS22.6-3) for that specimen. Transient pulse data and permeability determinations at sequentially increased effective pressures are shown in Figures 3 and 4, respectively, for samples saturated by distilled water or one of the 1 M brines. Transient pulse data illustrating changes in the rate of ($P_{up} - P_{dn}$) decay (and thus permeability k) with fluid

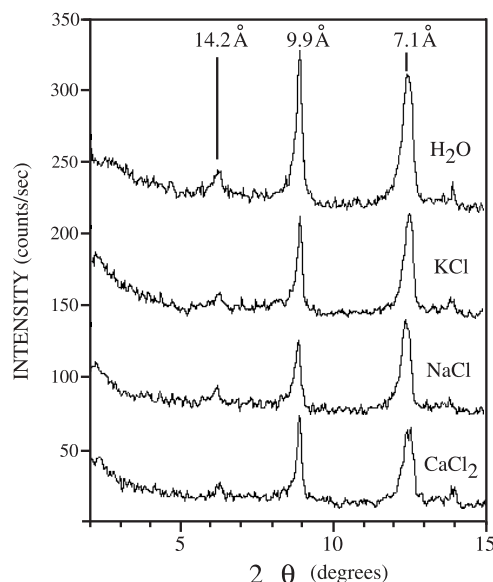


Figure 2. X-ray diffraction results for Wilcox shale powder samples immersed in distilled water, 1 M NaCl, 1 M KCl, and 1 M CaCl₂. Clay mineral diffraction peaks are apparent at 14.2 Å, 9.9 Å, and 7.1 Å due to (001) diffractions of chlorite, illite, and kaolinite, respectively, with little or no evidence for volumetric swelling of smectites.

Table 3. Permeability of Wilcox Shale to Fluids of Varying Composition

Sample	P_{cs} MPa	P_{ps} MPa	P_{es} MPa	Permeability, $\times 10^{-21} \text{ m}^2$	Pore Fluid
<i>Samples From Horizon 76A</i>					
WS22.6-1	13	10	3	219.3 (± 2.6)	H ₂ O, distilled
WS22.6-2	15	10	5	97.4 (± 0.6)	H ₂ O, distilled
WS22.6-3	18	10	8	43.3 (± 0.4)	H ₂ O, distilled
WS22.5-1	13	10	3	267.8 (± 1.2)	1 M NaCl
WS22.5-2	15	10	5	89.9 (± 0.8)	1 M NaCl
WS22.5-3	18	10	8	29.6 (± 0.2)	1 M NaCl
WS22.4-1	13	10	3	185.3 (± 2.2)	1 M KCl
WS22.4-2	15	10	5	83.4 (± 1.3)	1 M KCl
WS22.4-3	18	10	8	30.1 (± 0.3)	1 M KCl
<i>Samples From Horizon 76B</i>					
WS22.7-1	13	10	3	218.3 (± 3.2)	1 M NaCl
WS22.7-2	15	10	5	101.4 (± 1.9)	1 M NaCl
WS22.7-3	18	10	8	55.9 (± 0.7)	1 M NaCl
WS22.8-1	13	10	3	1043.7 (± 20)	1 M CaCl ₂
WS22.8-2	15	10	5	543.9 (± 5.8)	1 M CaCl ₂
WS22.8-3	18	10	8	224.1 (± 2.2)	1 M CaCl ₂
WS22.9-1	13	10	3	848.1 (± 5.8)	1 M CaCl ₂
WS22.9-2	15	10	5	355 (± 3.9)	1 M CaCl ₂
WS22.9-3	18	10	8	138.2 (± 0.8)	1 M CaCl ₂

composition are shown in Figures 5 and 6 for individual samples subjected to fluid exchange between transient pulse tests.

3.1. Volumetric Expansion

[20] Changes in rectangular specimen dimensions upon fluid saturation indicate that Wilcox shale is transversely isotropic with expansion perpendicular to bedding (*z*) greater than expansions parallel to bedding (in either *x* or *y* directions, Figure 1). Specimens saturated by 1 M CaCl₂ solution show the largest increase in volume (with strains in *x*, *y*, and *z* directions summing to 2.19%). Specimens saturated by 1 M KCl solution show the smallest volumetric expansion (of 0.77%), and specimens saturated by distilled water and 1 M NaCl show comparable, intermediate volumetric expansions (of 1.56% and 1.61%, respectively).

[21] Despite the macroscopic swelling measured for rectangular samples, X-ray diffraction patterns of powder samples in H₂O, and 1 M solutions of NaCl, KCl, and CaCl₂ show little change in clay basal plane spacings (Figure 2). Diffraction peaks due to (001) planes of kaolinite (7.1 Å), chlorite and smectites (14.2 Å), and illite (9.9 Å) show little variation in position, relative intensity, or width beyond variations associated with modal heterogeneity and

Table 4. Permeability of Wilcox Shale Upon Pore Fluid Exchange

Sample	P_{cs} MPa	P_{ps} MPa	P_{es} MPa	Permeability, $\times 10^{-21} \text{ m}^2$	Pore Fluid
<i>Sample From Horizon 76C</i>					
WS22.25-1	13	10	3	288.2 (± 2.8)	1 M NaCl
WS22.25-2	13	10	3	684.6 (± 5.1)	1 M CaCl ₂
WS22.25-3	13	10	3	614.3 (± 4.9)	1 M NaCl
<i>Sample From Horizon 76D</i>					
WS22.68.1-1	13	10	3	83.7 (± 1.8)	H ₂ O, distilled
WS22.68.1-2	13	10	3	86.3 (± 0.9)	1 M NaCl
WS22.68.1-3	13	10	3	56.6 (± 0.9)	H ₂ O, distilled

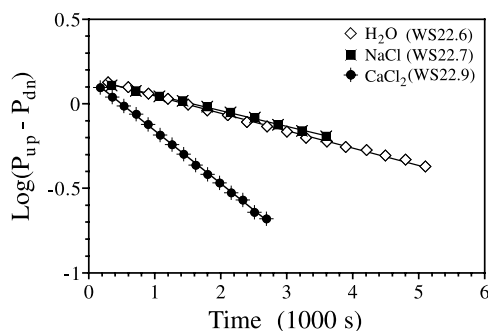


Figure 3. Results of transient pulse experiments performed on Wilcox shale specimens saturated by distilled water (WS22.6 from horizon 76A), 1 M NaCl (WS22.7 from horizon 76B), and 1 M CaCl₂ (WS22.9 from horizon 76B). The decay of the fluid pressure difference ($P_{up} - P_{dn}$) across the specimen length, plotted as $\log(P_{up} - P_{dn})$ versus time yields permeability k by way of the slope ($-\theta/2.303$) and equation (1). Specimens saturated by 1 M CaCl₂ exhibit higher ($P_{up} - P_{dn}$) decay rates than do specimens saturated by the other fluids with a steeper negative slope corresponding to higher permeability.

nonuniform clay orientations. In the absence of any shift or growth in the diffraction at 14.2 Å, we assign this peak to chlorite and conclude that smectites and mixed layer clays have negligible concentrations. The lack of evidence for clay swelling suggests that the macroscopic volume changes

measured upon saturation represent intergranular expansion processes.

3.2. Permeability

[22] Permeabilities determined for samples selected from each of two horizons (76A and 76B, chosen for lithologic similarity) and saturated by different pore fluids indicate that bedding-parallel fluid transport depends on fluid composition. The largest permeabilities were measured for two samples (from 76B) saturated by 1 M CaCl₂ and the smallest values of k were measured for a sample (from 76A) saturated by 1 M KCl (Table 3).

[23] In all transient pulse experiments reported, fluid pressure differences ($P_{up} - P_{dn}$) imposed across the ends of a cylindrical specimen at the beginning of each experiment were observed to decay according to equation (1), yielding a slope ($= -\theta/2.303$) in $\log(P_{up} - P_{dn})$ versus time that is linearly related to permeability k . At a given pressure, transient pulse experiments for samples saturated by 1 M CaCl₂ exhibit the most rapid decay in ($P_{up} - P_{dn}$), with k values that are greater, by factors of 3–5, than k of a comparable sample (from the same horizon, 76B) saturated by 1 M NaCl (Figure 3). While some variability in permeability was noted for samples (from a single horizon, 76A) saturated by distilled water, 1 M NaCl, and 1 M KCl, values of k for transport of these fluids through Wilcox shale differ by only $\sim 20\%$. Similar variation in permeability is apparent between specimens WS22.5 and WS22.7 taken from the two horizons (76A and 76B, respectively) and saturated by the same fluid (1 M NaCl).

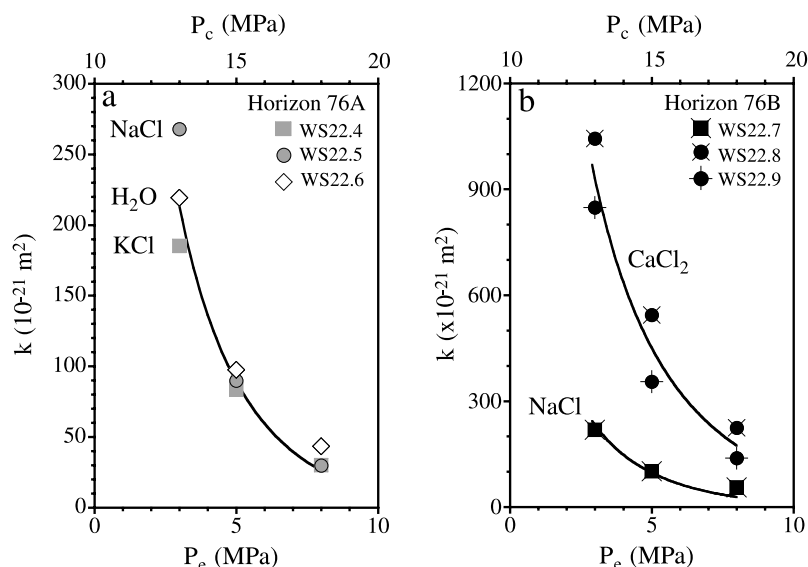


Figure 4. Bedding-parallel permeabilities k of Wilcox shale specimens saturated by distilled water, 1 M NaCl, 1 M KCl, and 1 M CaCl₂ and subjected to systematically increasing effective pressure P_e . (a) Specimens taken from the same lithologic horizon (76A) and saturated by distilled water and 1 M NaCl and KCl solutions show similar reductions in permeability with increasing effective pressure; all can be fit satisfactorily by a single cubic law (equation (2)) where $k_0 = 13.2 \times 10^{-18} \text{ m}^2$, $m = 0.166$ and $P_1 = 18.4 \text{ MPa}$. (b) Specimens taken from horizon 76B and saturated by 1 M NaCl and 1 M CaCl₂ show that permeability depends on fluid composition with significantly higher k for the transport of 1 M CaCl₂ than k for transport of the other fluids. The results for 1 M CaCl₂, best fit to the cubic k - P_e law (equation (2)), yields a reference $k_0 = 40 \times 10^{-18} \text{ m}^2$, much higher than k_0 determined for the other fluids, and parameters $m = 0.161$ and $P_1 = 24.2 \text{ MPa}$ that are comparable to m and P_1 determined for the other fluids.

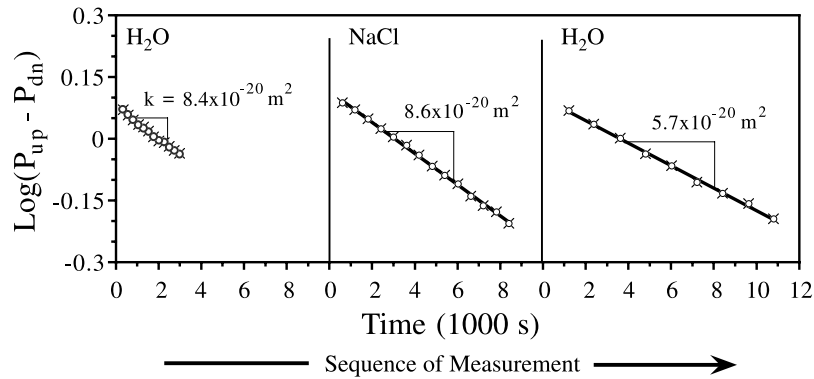


Figure 5. Results of sequential transient pulse experiments performed on Wilcox shale specimen WS22.68.1, saturated first by distilled water, then by 1 M NaCl, and again by distilled water. Permeabilities determined from the slopes in $\log(P_{up} - P_{dn})$ versus time in the first two experiments are the same within error, yet the permeability determined in the third experiment (for the same sample, returned to distilled water) is significantly lower than determined in the first two experiments.

[24] Sequential measurements of bedding-parallel k with increasing effective pressure reveal nonlinear k - P_e relationships (Figure 4) that can be fit satisfactorily by the cubic law, equation (2) for transport of all pore fluids tested. Given that permeabilities measured for transport of distilled water and 1 M KCl are similar to those for 1 M NaCl, we adopt the best fit values

$$m = 0.166$$

$$P_1 = 18.4 \text{ MPa}$$

determined for the larger data set of Kwon *et al.* [2004] for bedding-parallel flow of 1 M NaCl in low clay content specimens, and find a mean value of

$$k_0 = 13.2(\pm 2.4) \times 10^{-18} \text{ m}^2$$

for transport of water, 1 M KCl and 1 M NaCl in these experiments (Figure 4a). This value is somewhat larger than the reference permeability $k_0 = 11.8 \times 10^{-18} \text{ m}^2$ determined

by Kwon *et al.* [2004] for the 1 M NaCl transport data, but it falls well within the standard deviation ($\pm 3.4 \times 10^{-18} \text{ m}^2$) determined for similar, low clay content Wilcox shale samples. In contrast, permeabilities measured for the transport of 1 M CaCl_2 at any given pressure are significantly higher than for 1 M NaCl (Figure 4b), and independent regressions to the 1 M CaCl_2 data yield

$$k_0 = 40(\pm 8) \times 10^{-18} \text{ m}^2,$$

$$m = 0.161(\pm 0.004),$$

$$P_1 = 24.2(\pm 6) \text{ MPa}.$$

The value of m determined for 1 M CaCl_2 is indistinguishable from that determined for bedding-parallel flow of 1 M NaCl through low clay content samples and P_1 is only slightly larger than the best fit value for 1 M NaCl transport. Higher values of k for 1 M CaCl_2 transport can largely be accounted for by the value of k_0 , which is four times larger

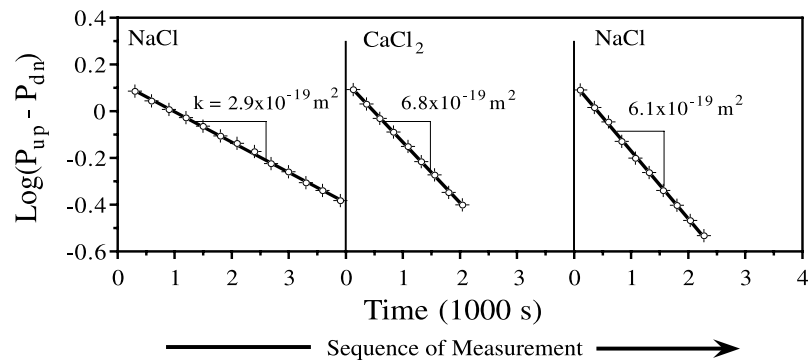


Figure 6. Results of sequential transient pulse experiments performed on Wilcox shale specimen WS22.25, saturated first by 1 M NaCl, then by 1 M CaCl_2 , and again by 1 M NaCl. Permeabilities determined from the slopes in $\log(P_{up} - P_{dn})$ versus time exhibit a significant increase in k for this sample when the NaCl solution is replaced by the CaCl_2 solution, yet permeability does not return to the original value when the sample is again saturated by the NaCl solution.

than the reference permeability determined for 1 M NaCl transport.

[25] Given the small differences in k for distilled water and 1 M solutions of NaCl and KCl, and the sample-to-sample variations noted for Wilcox shale, even for samples taken from the same stratigraphic horizon, we decided to do multiple permeability experiments on individual specimens, changing the fluid composition between transient pulse tests. However, these experiments were not successful in resolving differences in k for bedding-parallel flow of water, 1 M NaCl, and 1 M KCl. Instead, they reveal irreversible changes in permeability related to the specimen's prior exposure to fluids of differing composition.

[26] Sequential transient pulse experiments performed on sample WS22.68.1, saturated first with distilled water, then with 1 M NaCl, and again with distilled water exhibit similar ($P_{\text{up}} - P_{\text{dn}}$) decay rates in the first two experiments and a significantly lower decay rate in the final experiment (Figure 5). Permeabilities for distilled H₂O and 1 M NaCl in the first two experiments ($k = 83.7 \times 10^{-21} \text{ m}^2$ and $86.3 \times 10^{-21} \text{ m}^2$, respectively) are indistinguishable at the 10% level, yet the permeability for H₂O in the final experiment ($k = 56.6 \times 10^{-21} \text{ m}^2$) appears to have been lowered significantly by the specimen's prior exposure to the NaCl solution.

[27] Sequential transient pulse experiments performed on sample WS22.25, saturated first with 1 M NaCl, then with 1 M CaCl₂, and again with 1 M NaCl show remarkable changes in permeability that are irreversible. Permeability of this specimen increased markedly upon saturation by 1 M CaCl₂ (with k increasing from $288 \times 10^{-21} \text{ m}^2$ in the first 1 M NaCl experiment to $685 \times 10^{-21} \text{ m}^2$ after the same sample was saturated by 1 M CaCl₂) and remained high ($k = 614 \times 10^{-21} \text{ m}^2$) when the sample was saturated again by 1 M NaCl (Figure 6). Despite our best efforts to exchange pore fluids of these specimens with a new fluid of differing composition between sequential transient pulse experiments, permeabilities appear to depend on the specimen's history of fluid saturation and exposure to different cations.

4. Discussion

[28] Wilcox shale specimens exhibit volumetric expansion and transport properties that depend on fluid composition along similar trends. The largest volumetric expansions are observed for specimens immersed in 1 M CaCl₂, with volume change dominated by expansion perpendicular to bedding (Figure 1). Similarly, the largest bedding-parallel permeabilities at a given P_e are measured for 1 M CaCl₂ (Figure 4). Volumetric expansions and permeabilities of specimens saturated by 1 M NaCl and distilled water are comparable, while volumetric expansions of specimens saturated by 1 M KCl are small and permeabilities for 1 M KCl are arguably smaller than permeabilities measured for the other fluids.

4.1. Influence of Fluid Chemistry on Expansion

[29] Argillaceous rocks and clay aggregates are commonly observed to expand when immersed in aqueous fluids or exposed to humidity at ambient pressure [e.g., Henkel, 1959; Chugh et al., 1981; Huang et al., 1986a; Harrington et al., 2001]. When volume is held constant, fluid saturation may

generate swelling pressures [Huang et al., 1986b; Steiger, 1993], with swelling potential attributed to clay mineralogy [Madsen and Muller-Vonmoos, 1985] and swelling of clays with variable basal (001) dimensions [Van Olphen and Fripiat, 1979]. In the absence of X-ray diffraction results, the bulk expansions measured for Wilcox shale specimens immersed in distilled water and the three brines could be explained by clay swelling. Anisotropy in expansion could be explained by the preferred orientation of clay platelets parallel to bedding, and differences in volumetric expansion for the different fluids could be explained by cation exchange between the fluid and clay mineral interlayers and consequent changes in swelling potential. However, X-ray diffraction measurements (Figure 2) show no shifts in basal diffraction peaks of the clay minerals or any diffraction broadening. Thus the concentrations of smectites and mixed layer clays must be small, and intracrystalline swelling of clay minerals is negligible.

[30] Alternatively, swelling of Wilcox shale may be due to dimensional changes in the clay mineral-fluid interface. Exchange of cations between clays and the fluid may alter the inner sphere complexes of clay surfaces and the adjacent diffuse ion layer of the fluid [Sposito et al., 1999] leaving interlayer complexes unchanged. Much of the anisotropic swelling of Opalinus clay [Harrington et al., 2001] has been associated with opening of oriented cracks. Given our bulk expansion and X-ray diffraction results, we suspect that Wilcox shale expands by similar dilatant, intergranular processes. If so, anisotropy in bulk expansion measurements may be explained by opening crack-like voids (type I and II) [Kwon et al., 2004] which are preferentially aligned with bedding.

4.2. Influence of Fluid Chemistry on Permeability

[31] Permeabilities of Wilcox shale for bedding-parallel flow of 1 M CaCl₂ are 3–5 times greater than those measured for the other fluids. Previous studies of transport properties of clay aggregates and clay-bearing sandstones have shown that permeabilities are higher for CaCl₂ solutions than for electrolyte solutions with monovalent cations or for water [Mesri and Olson, 1971; Olsen, 1972; Lever and Dawe, 1984]. However, in contrast with our permeability results for distilled water and 1 M NaCl and KCl solutions in shale, studies of swelling clay aggregates and clay-bearing sandstones saturated by water and NaCl solutions of varying concentration have shown that permeability depends on ionic strength. Swelling clays and clay-bearing sandstones initially saturated by a NaCl solution and then exposed to an influx of distilled water exhibit reductions in permeability with cumulative flow of distilled water [Mungan, 1965; Moore et al., 1982]. Similarly, permeabilities of clay-bearing Berea sandstone decrease as the concentration of NaCl is decreased below a threshold concentration [Jones, 1964; Khilar and Fogler, 1983].

[32] Permeability reductions of swelling clay aggregates exposed to distilled water have been attributed to clay mineral expansion and resulting pore aperture reductions [Mesri and Olson, 1971; Olsen, 1972; Van Olphen, 1977; Moore et al., 1982; Whitworth and Fritz, 1994]. However, this mechanism seems unlikely for Wilcox shale given the absence of significant clay swelling. Permeability reduc-

tions of clay-bearing sandstones exposed to water have been attributed to clay mineral expansion, dispersion of fine clays within the pore fluid by repulsive surface forces, and blockage of pore throats by clays that are redistributed by pore fluid flow [Hewitt, 1963; Jones, 1964; Mungan, 1965, 1968; Gray and Rex, 1966; Khilar and Fogler, 1981, 1983; Kia et al., 1987]. Compared with the dimensions of pores in sandstones (i.e., $\sim 150 \mu\text{m}$ for Berea sandstone) [Weinbrandt and Fatt, 1970], voids observed in Wilcox shale are extremely small, with minimum dimensions of crack-like and irregular voids (from 1 nm to $3 \mu\text{m}$) that are comparable to the dimensions of clay platelets themselves [Kwon et al., 2004]. As a result, clays cannot become suspended and move within the pore space, as they can in clay-bearing sandstones. We conclude that the mechanisms by which permeability depends on pore fluid composition in Wilcox shale differs from those in aggregates of swelling clays and clay-bearing sandstones.

[33] In studies of Wilcox shale permeability using a 1 M NaCl solution [Kwon et al., 2001, 2004], we found that reductions in k with increasing effective pressure P_e can be described by a modified cubic law (2) where values of the reference permeability k_0 depend on flow direction and clay content, values of the exponent m depend on flow direction, and values of P_1 are nearly the same for different flow directions and clay contents. Best fits of the 1 M CaCl_2 permeability data of this study to (2) indicate that high permeabilities for this pore fluid are associated with a reference permeability ($k_0 = 40 \times 10^{-18} \text{ m}^2$) that is large compared with k_0 for bedding-parallel flow of the other fluids ($k_0 = 13.2 \times 10^{-18} \text{ m}^2$, determined as an average value for distilled water and 1 M solutions of NaCl and KCl). Remarkably, values of m ($= 0.161$) and P_1 ($= 24.2 \text{ MPa}$) determined for 1 M CaCl_2 are indistinguishable from those ($m = 0.166$, $P_1 = 18.4 \text{ MPa}$) used to fit the 1 M NaCl, 1 M KCl, and distilled water results.

[34] For a given fluid, the fit of permeabilities at elevated P_e to the cubic law can be explained if fluid conduits are crack-like in their dimensions and properties. On the basis of the physical model used to derive equation (2), k_0 depends on the extent, geometry, and connectedness of the pore space at the reference state ($P_e = 0$), while parameters m and P_1 depend on pore geometries and properties that describe the response of pores to increasing effective pressure P_e . The dependence of k_0 on fluid composition therefore corresponds to changes in the pore network capable of carrying fluid parallel to bedding.

[35] Parameters m and P_1 are insensitive to fluid chemistry, consistent with their physical interpretation as terms describing the geometry and properties of solid asperities of conduit surfaces; m is related to the height distribution of asperities and P_1 is an effective modulus of those asperities. The similarity of parameters m and P_1 for 1 M CaCl_2 and for the other fluids indicate that conduit characteristics are little affected by pore fluid. Processes of clay mineral dispersion and redistribution within the connected pore space, as observed in clay-bearing sandstones, would likely alter conduit asperity geometries where clays are removed and deposited. Thus these processes are ruled out.

[36] We conclude that the dependence of permeability on fluid chemistry results from changes in the fluid-clay interface and consequences for the capacity of the

connected pore space to transmit fluid. These changes could involve dimensional changes or electro-osmotic coupling.

[37] Faulkner and Rutter [2000] explained differences in permeability of clay-bearing fault gouge to flow of water and argon by way of dimensional changes in pores. X-ray diffraction results for fault gouge from the Carboneras fault zone (Spain) showed little evidence of clay swelling upon saturation by water, with layer silicates consisting of muscovite/illite and chlorite. Despite the absence of smectites or mixed layer clays, Faulkner and Rutter [2000] found that permeabilities for water are an order of magnitude smaller than permeabilities for argon. They argued that the effective apertures of pores for fluid flow are smaller when aqueous fluids interact with the solid to form static nanometer dimension interfacial layers of structured water between solid conduit walls. Likewise, our specimens saturated by aqueous fluids fail to show clay mineral swelling; yet, we observe bulk expansions and permeabilities that are larger for specimens saturated by 1 M CaCl_2 solution than for specimens saturated by distilled water or 1 M solutions of NaCl and KCl.

[38] Basal surfaces of clay minerals in contact with fluids of circumneutral pH carry a net negative charge as a result of isomorphic substitutions of cations of high valence by cations of lower valence [Van Olphen, 1977; Sposito, 1984; McBride, 1989; Sparks, 1995]. The net negative layer charge is compensated by counterions, which are electrostatically attracted to the charged surface layer, within the adjacent liquid. These compensating cations occupy a diffuse surface layer outside of the inner surface layer, extending into the solution. The inner charged interface and part of the outer diffuse layer is static and can be distinguished from the free fluid phase. On the basis of diffuse double-layer theory, we expect that low counterion valences, low electrolyte concentrations, or a high dielectric constant of the solvent can increase the thickness of the electric double layer, as well as the static, immobile water at clay-fluid interfaces [Van Olphen, 1977; Sposito, 1984; Singh and Uehara, 1986; McBride, 1989; Sparks, 1995]. When adjacent clay surfaces are very close to each other, the fluid film between the crystalline solids may take on an ordered structure [Pashley and Israelachvili, 1984; Israelachvili, 1992] and exhibit a plastic threshold to flow [Israelachvili, 1986; Israelachvili and Kott, 1989; Gee et al., 1990] unlike the viscous response of the same pore fluid far from solid-fluid interfaces.

[39] Our permeability results for fluids of varying composition in Wilcox shale may thus be explained qualitatively by changes in effective aperture of fluid conduits associated with dimensional changes in fluid-clay mineral interfaces. However, estimates of double-layer thickness for the high-salinity brines used in this study are much smaller than even the finest pores imaged (1–10 nm). Following Sparks [1995], a double-layer thickness of $\sim 0.18 \text{ nm}$ is predicted for the 1 M CaCl_2 solution as opposed to $\sim 0.3 \text{ nm}$ for the 1 M NaCl solution and the static, immobile fluid layer will be even thinner. Effective dimensions for fluid flow through pores $\geq 10 \text{ nm}$ are therefore expected to be similar for the CaCl_2 and NaCl solutions.

[40] The influence of fluid composition may instead be explained by differing surface charge effects on fluid flow for the different pore fluids. Revil and Leroy [2004] have

developed a model of ionic transport in shale which takes into account coupling between ionic fluxes, electrical current, heat flow, and fluid flow and their thermodynamic driving potentials. On the basis of this model, electro-osmotic coupling may influence fluid flow. High permeabilities for 1 M CaCl₂ relative to those measured for 1 M NaCl and 1 M KCl solutions can be explained by weaker electro-osmotic coupling for the 1 M CaCl₂ and less resistance to its flow than for the other pore fluids.

[41] In argillaceous rocks with swelling clays, intracrystalline expansions may be more important than they are in Wilcox shale, yet changes in the surficial double layer have been called upon to explain permeabilities of electrolyte solutions in smectite aggregates as well [Whitworth and Fritz, 1994]. We expect that the results obtained here represent an end-member with effects of fluid composition on the functionally connected pore space due solely to cation exchange at clay-fluid interfaces. The influence of fluid chemistry determined here should also hold for other shales and mudstones, but other processes may also become important if swelling clays are present. Multiple mechanisms may be responsible for changes in connected porosity if cation exchange occurs between the pore fluid, surficial clay double layers, and the clay mineral interlayers [Mesri and Olson, 1971; Olsen, 1972; Moore et al., 1982; Whitworth and Fritz, 1994; Sposito et al., 1999].

4.3. Nonrecoverable Cation Exchange

[42] Our original motivation for making multiple permeability measurements on specimens subjected to sequential changes in pore fluid composition was to eliminate sample-to-sample variations from our comparisons of k for different pore fluids. Instead, they serve to demonstrate that permeabilities change irreversibly with changes in fluid chemistry. Specimen WS22.68.1 subjected to the sequential flow of distilled H₂O, 1 M NaCl solution, and distilled H₂O exhibited nearly identical permeabilities in the first two experiments with distilled water and 1 M NaCl, but then showed a decrease in k when distilled water was reintroduced following saturation by 1 M NaCl (Figure 5). Specimen WS22.25 subjected to sequential flow of 1 M NaCl, 1 M CaCl₂, and 1 M NaCl exhibited an increase in permeability when 1 M CaCl₂ replaced the 1 M NaCl solution, but k remained constant when CaCl₂ pore fluid was replaced by inflowing 1 M NaCl solution (Figure 6).

[43] Complex variations in permeability associated with changes in incoming fluid composition have also been observed for clay aggregates and clay-bearing sandstones. While the processes by which fluid composition influences permeability of these materials may differ, the nonrecoverable changes that have been observed are generally consistent with results of our fluid exchange experiments. Significant decreases in k have been observed for swelling clay aggregates [Moore et al., 1982] when pore fluids consisting of NaCl solution are displaced by incoming distilled water. Reductions in permeability have likewise been observed for clay-bearing sandstones subjected to an influx of distilled water following saturation by NaCl and KCl solutions [Gray and Rex, 1966; Mungan, 1965, 1968; Khilar and Folger, 1983; Lever and Dawe, 1984]. In fluid exchange experiments performed on Berea sandstone, Mungan [1968] reversed the sequence of incoming fluid

composition, beginning with distilled water, followed by a brine, and then reintroducing distilled water. In these experiments, Mungan [1968] found that permeability is unchanged when distilled water is replaced by a NaCl solution, much as we observe for Wilcox shale, but that permeability drops when the inflowing fluid is changed back to distilled water. Mungan [1968] went further to show that the same path-dependent effects can be observed when pore water is replaced by KCl or NaBr solutions and the incoming fluid is changed back to distilled water. However, when fully reversed fluid exchange experiments were done with distilled water, followed by a CaCl₂ or AlCl₃ solution, and then followed by distilled water, no changes in permeability were noted.

[44] When ions of different valence are present in solution, the diffuse double-layer of clays may exhibit differential adsorption properties and ion selectivity [Bolt, 1955; Jones, 1964; Grim, 1968; Kharaka and Berry, 1973; Sposito, 1984]. Nonrecoverable changes in permeability of Wilcox shale during our sequential flow experiments can be explained by preferential adsorption of high valence cations to clay surfaces. Divalent ions are concentrated in the double layer to a greater extent relative to the bulk fluid composition than are monovalent ions [Singh and Uehara, 1986].

[45] Despite our attempts to exchange several pore volumes of fluid with these shale specimens, the path-dependent changes in permeability suggest that cation exchange was not reversed. Differences in cation adsorption to clay mineral surfaces may lead to differences in cation mobility relative to the advective flow of pore fluid [Kharaka and Berry, 1973] with mobilities of Li and Na in solution that are higher than determined for K ions in a number of different types of clays, and lower mobilities determined for Ca and other divalent cations. If clays of Wilcox shale have substantial quantities of K, and potentially smaller quantities of Na, adsorbed at their surfaces, influx of distilled water in the first series of fluid exchange experiments, performed on sample WS22.68.1 (Figure 5), may not readily strip these ions from clay mineral surfaces. Upon saturation by the NaCl solution, exchange of K and Na may have occurred at clay-fluid interfaces without altering the electrical character of the interfaces. However, upon reintroduction of distilled water, Na ions may enter the mobile pore fluid and change the clay interface chemistry.

[46] The irreversible increase in permeability with the introduction of 1 M CaCl₂ in the second series of fluid exchange experiments, performed on sample WS22.25 (Figure 6), may be explained if monovalent Na cations are replaced by divalent Ca ions, leading either to a reduction in double-layer thickness or to a reduction in electro-osmotic coupling. Given that Ca ions are strongly adsorbed to clay surfaces, exchange of Ca and Na at clay surfaces may have been limited when NaCl solution was reintroduced, leaving fluid transport properties unchanged.

5. Conclusions

[47] Experimental measurements of permeability, bulk expansion, and X-ray diffraction on Wilcox shale specimens saturated by distilled water and 1 M solutions of NaCl, KCl, and CaCl₂ lead to the following conclusions:

[48] 1. Bedding-parallel permeabilities for flow of 1 M CaCl₂ are 3–5 times greater than measured for the transport of distilled water or 1 M solutions of NaCl or KCl.

[49] 2. Permeabilities determined for all of the pore fluids tested depend on effective pressure P_e by a modified cubic law $k = k_0 [1 - (P_e/P_1)^m]^3$, where k_0 depends on fluid chemistry ($k_0 = 40 \times 10^{-18} \text{ m}^2$ for 1 M CaCl₂ while $k_0 = \sim 13 \times 10^{-18} \text{ m}^2$ for distilled water, 1 M NaCl, and 1 M KCl) and m and P_1 are insensitive to pore fluid composition ($0.161 \leq m \leq 0.166$; $18 \leq P_1 \leq 24 \text{ MPa}$), depending instead on fluid conduit geometry and properties.

[50] 3. Bulk expansion of Wilcox shale upon fluid saturation depends on the composition of the fluid, with changes in volume dominated by expansion perpendicular to bedding. The largest volumetric expansions are observed for specimens saturated by 1 M CaCl₂, while comparable expansions are observed for distilled water and 1 M NaCl, and the lowest expansions are observed for 1 M KCl.

[51] 4. The reference permeability k_0 appears to depend on fluid composition through cation exchange at clay-fluid interfaces, particularly when divalent cations replace adsorbed monovalent cations, and alter the electrical double layer.

[52] 5. Permeability changes with changing fluid chemistry are path-dependent and appear to be due to differential adsorption and cation selectivity of clay surfaces.

[53] **Acknowledgments.** This study benefited from discussions with Anthony Gangi, Brann Johnson, and David Wiltschko and from critical reviews by Andre Revil, Ian Main, Jack Thomas, and an anonymous reviewer. We are thankful to Robert Berg for generously providing the Wilcox shale core for use in this study. We thank Jack Magouirk for technical support throughout this study. This study was supported by the U.S. Department of Energy, Office of Basic Energy Sciences, Division of Chemical Sciences, Geosciences and Biosciences under grant DE-FG05-87ER13711.

References

- Addis, M. A., and M. E. Jones (1985), Volume changes during diagenesis, *Mar. Pet. Geol.*, **2**, 241–246.
- Barker, C. (1972), Aquathermal pressuring - role of temperature in development of abnormal-pressure zones, *Am. Assoc. Pet. Geol. Bull.*, **56**, 2068–2071.
- Barker, C. (1987), Development of abnormal and subnormal pressures in reservoirs containing bacterially generated gas, *AAPG Bull.*, **71**, 1404–1413.
- Barker, C. (1990), Calculated volume and pressure changes during the thermal cracking of oil to gas in reservoirs, *AAPG Bull.*, **74**, 1254–1261.
- Berg, R. R. (1975), Capillary pressures in stratigraphic traps, *AAPG Bull.*, **59**, 939–956.
- Berg, R. R., and M. F. Habeck (1982), Abnormal pressures in the lower Vicksburg, McAllen ranch fields, south Texas, *Trans. Gulf Coast Assoc. Geol. Soc.*, **32**, 247–253.
- Bigelow, E. L. (1994), Global occurrences of abnormal pressures, in *Studies in Abnormal Pressures*, edited by W. H. Fertl, R. E. Chapman, and R. E. Hotz, pp. 1–17, Elsevier Sci., New York.
- Bjorlykke, K., and K. Gran (1994), Salinity variations in North Sea formation waters: Implications for large-scale fluid movements, *Mar. Pet. Geol.*, **11**, 5–9.
- Bolt, G. H. (1955), Ion adsorption by clays, *Soil Sci.*, **79**, 267–276.
- Brace, W. F., J. B. Walsh, and W. T. Frangos (1968), Permeability of granite under high pressure, *J. Geophys. Res.*, **73**, 2225–2236.
- Bradley, J. S. (1975), Abnormal formation pressure, *AAPG Bull.*, **59**, 957–973.
- Bredehoeft, J. D., and B. B. Hanshaw (1968), On the maintenance of anomalous fluid pressures, I, Thick sedimentary sequences, *Geol. Soc. Am. Bull.*, **79**, 1097–1106.
- Bredehoeft, J. D., C. E. Neuzil, and P. C. D. Milly (1983), Regional flow in the Dakota aquifer - A study of the role of confining layers, *U.S. Geol. Surv. Water Supply Pap.*, **2237**, 45 pp.
- Burst, J. F. (1969), Diagenesis of Gulf Coast clayey sediments and its possible relation to petroleum migration, *Am. Assoc. Pet. Geol. Bull.*, **53**, 73–93.
- Chapman, R. E. (1972), Clays with abnormal interstitial fluid pressures, *Am. Assoc. Pet. Geol. Bull.*, **56**, 790–795.
- Chapman, R. E. (1982), Mechanical versus thermal cause of abnormally high pore pressures in shales—Reply, *AAPG Bull.*, **66**, 101–102.
- Chapman, R. E. (1994), The geology of abnormal pore pressures, in *Studies in Abnormal Pressures*, edited by W. H. Fertl, R. E. Chapman, and R. E. Hotz, pp. 19–49, Elsevier Sci., New York.
- Chilingarian, G. V., H. H. Rieke, and A. Kazi (1994), Chemistry of pore water, in *Studies in Abnormal Pressures*, edited by W. H. Fertl, R. E. Chapman, and R. E. Hotz, pp. 107–153, Elsevier Sci., New York.
- Chugh, Y. P., A. Okunola, and M. Hall (1981), Moisture absorption and swelling behavior of the Dykersburg shale, *Trans. Soc. Min. Eng.*, **268**, 1808–1812.
- Deming, D. (1994), Factors necessary to define a pressure seal, *AAPG Bull.*, **78**, 1005–1009.
- Dewhurst, C. N., A. C. Aplin, J.-P. Sarda, and Y. Yang (1998), Compaction-driven evolution of porosity and permeability in natural mudstones: An experimental study, *J. Geophys. Res.*, **103**, 651–661.
- Dewhurst, C. N., A. C. Aplin, and J.-P. Sarda (1999), Influence of clay fraction on pore-scale properties and hydraulic conductivity of experimentally compacted mudstones, *J. Geophys. Res.*, **104**, 29,261–29,274.
- Dickey, P. A., C. R. Shriram, and W. R. Paine (1968), Abnormal pressures in deep wells of southwestern Louisiana, *Science*, **160**, 609–615.
- Dickinson, G. (1953), Geological aspects of abnormal reservoir pressures in Gulf Coast Louisiana, *Am. Assoc. Pet. Geol. Bull.*, **37**, 410–432.
- Dzevanishir, R. D., L. A. Buryakovskiy, and G. V. Chilingarian (1986), Simple quantitative evaluation of porosity of argillaceous sediments at various depths of burial, *Sediment. Geol.*, **46**, 169–175.
- Faulkner, D. R., and E. H. Rutter (2000), Comparisons of water and argon permeability in natural clay-bearing fault gouge under high pressure at 20°C, *J. Geophys. Res.*, **105**, 16,415–16,426.
- Fournier, R. O., and A. H. Truesdell (1973), An empirical Na-K-Ca geothermometer for natural waters, *Geochim. Cosmochim. Acta*, **37**, 1255–1275.
- Freed, R. L., and D. R. Peacor (1989), Geopressed shale and sealing effect of smectite to illite transition, *AAPG Bull.*, **73**, 1223–1232.
- Gangi, A. F. (1978), Variation of whole and fractured porous rock permeability with confining pressure, *Int. J. Rock Mech. Min. Sci.*, **15**, 249–257.
- Gee, M. L., P. M. McGuiggan, J. N. Israelachvili, and A. M. Homola (1990), Liquid to solid like transitions of molecularly thin films under shear, *J. Chem. Phys.*, **93**, 1895–1906.
- Gray, D. H., and R. W. Rex (1966), Formation damage in sandstones caused by clay dispersion and migration, in *14th National Conference on Clays and Clay Minerals*, pp. 355–366, Realigraf, Madrid, Spain.
- Green, D. H., and H. F. Wang (1986), Fluid pressure response to undrained compression in saturated sedimentary rock, *Geophysics*, **51**, 948–956.
- Grim, R. E. (1968), *Clay Mineralogy*, 2nd ed., 596 pp., McGraw-Hill, New York.
- Hanor, J. S. (1994), Physical and chemical controls on the composition of waters in sedimentary basins, *Mar. Pet. Geol.*, **11**, 31–45.
- Hao, S., Z. Huang, G. Liu, and Y. Zheng (2000), Geophysical properties of cap rocks in Qiongdongnan Basin, South China Sea, *Mar. Pet. Geol.*, **17**, 547–555.
- Harrington, J. F., S. T. Horseman, and D. J. Noy (2001), Swelling and osmotic flow in a potential host rock, in *Proceedings of the 6th International Workshop on Key Issues in Waste Isolation Research (KIWAR)*, edited by P. Delage, pp. 169–188, Ecole Natl. des Ponts et Chaussées, Paris, 28–30 Nov.
- Harrison, W. J., and L. L. Summa (1991), Paleohydrology of the Gulf of Mexico basin, *Am. J. Sci.*, **291**, 109–176.
- Hart, B. S., P. B. Flemings, and A. Deshpande (1995), Porosity and pressure: Role of compaction disequilibrium in the development of geopressures in a Gulf Coast Pleistocene basin, *Geology*, **23**, 45–48.
- Hedberg, H. D. (1974), Relation of methane generation to undercompacted shales, shale diapirs and mud volcanoes, *AAPG Bull.*, **58**, 661–673.
- Henkel, D. J. (1959), The relationships between the strength, pore-water pressure, and volume-change characteristics of saturated clays, *Geotechnique*, **9**, 119–135.
- Hewitt, C. H. (1963), Analytical techniques for recognizing water sensitive reservoir rocks, *J. Pet. Technol.*, **15**, 813–818.
- Hower, J., E. V. Eslinger, M. E. However, and E. D. Perry (1976), Mechanism of burial metamorphism of argillaceous sediment, I. Mineralogical and chemical evidence, *Geol. Soc. Am. Bull.*, **87**, 725–737.
- Huang, S. L., N. B. Aughenbaugh, and J. D. Rockaway (1986a), Characterization of swelling potential of shale strata, *Proc. U.S. Symp. Rock Mech.*, **27th**, 68–76.

- Huang, S. L., N. B. Aughenbaugh, and J. D. Rockaway (1986b), Swelling pressure studies of shales, *Int. J. Rock Mech. Min. Sci.*, **23**, 371–377.
- Hunt, J. M. (1990), Generation and migration of petroleum from abnormally pressured fluid compartments, *AAPG Bull.*, **74**, 1–12.
- Ibanez, W. D., and A. K. Kronenberg (1993), Experimental deformation of shale: Mechanical properties and microstructural indicators of mechanisms, *Int. J. Rock Mech. Min. Sci.*, **30**, 723–734.
- Illing, V. C. (1938), The origin of pressure in oil pools, in *The Science of Petroleum*, vol. 1, edited by A. E. Dunstan, pp. 224–229, Oxford Univ. Press, New York.
- Israelachvili, J. N. (1986), Measurements of the viscosity of liquids in very thin films, *J. Colloid Interface Sci.*, **110**, 263–271.
- Israelachvili, J. N. (1992), Adhesion forces between surfaces in liquids and condensable vapors, *Surface Sci. Rep.*, **14**, 109–159.
- Israelachvili, J. N., and S. J. Kott (1989), Shear properties and structure of simple liquids in molecularly thin films: The transition from bulk (continuum) to molecular behavior with decreasing film thickness, *J. Colloid Interface Sci.*, **129**, 461–467.
- Jones, F. O., Jr. (1964), Influence of chemical composition of water on clay blocking of permeability, *J. Pet. Technol.*, **16**, 441–446.
- Katsube, T. J., B. S. Mudford, and M. E. Best (1991), Petrophysical characteristics of shales from the Scotian Shelf, *Geophysics*, **56**, 1681–1689.
- Kharaka, Y. K., and F. A. F. Berry (1973), Simultaneous flow of water and solutes through geological membranes - I. experimental investigation, *Geochim. Cosmochim. Acta*, **37**, 2577–2603.
- Kharaka, Y. K., E. Callender, and R. H. Wallace Jr. (1977), Geochemistry of geopressured geothermal waters from the Frio clay in the Gulf Coast region of Texas, *Geology*, **5**, 241–244.
- Khilar, K. C., and H. S. Fogler (1981), Permeability reduction in water sensitivity of sandstones, in *Surface Phenomena in Enhanced Oil Recovery*, edited by S. O. Shah, pp. 721–740, Plenum, New York.
- Khilar, K. C., and H. S. Fogler (1983), Water sensitivity of sandstones, *Soc. Pet. Eng. J.*, **23**, 55–64.
- Kia, S. F., H. S. Fogler, M. G. Reed, and R. N. Vaidya (1987), Effect of salt composition on clay release in Berea sandstones, *SPE Prod. Eng.*, **2**, 277–283.
- Kim, J.-W., W. R. Bryant, J. S. Watkins, and T. T. Tieh (1999), Electron microscopic observations of shale diagenesis, offshore Louisiana, USA, Gulf of Mexico, *Geo Mar. Lett.*, **18**, 234–240.
- Kwon, O., A. K. Kronenberg, A. F. Gangi, and B. Johnson (2001), Permeability of Wilcox shale and its effective pressure law, *J. Geophys. Res.*, **106**, 19,339–19,353.
- Kwon, O., A. K. Kronenberg, A. F. Gangi, B. Johnson, and B. E. Herbert (2004), Permeability of Illite-bearing shale: 1. Anisotropy and effects of clay content and loading, *J. Geophys. Res.*, **B10205**, doi:10.1029/2004JB003052.
- Land, L. S. (1995), Na-Ca-Cl saline formation waters, Frio Formation (Oligocene), south Texas, USA: Products of diagenesis, *Geochim. Cosmochim. Acta*, **59**, 2163–2174.
- Land, L. S., and G. L. Macpherson (1992), Origin of saline formation waters, Cenozoic section, Gulf of Mexico sedimentary basin, *AAPG Bull.*, **76**, 1344–1362.
- Lee, J. H., J. H. Ahn, and D. Peacor (1985), Textures in layered silicates: Progressive changes through diagenesis and low temperature metamorphism, *J. Sediment. Petrol.*, **55**, 532–540.
- Lever, A., and R. A. Dawe (1984), Water-sensitivity and migration of fines in the Hopeman sandstone, *J. Pet. Geol.*, **7**, 87–108.
- Lide, D. R. (1997), *CRC Handbook of Chemistry and Physics*, 78th ed., 1-62 pp., CRC Press, Boca Raton, Fla.
- Lin, W. (1978), Measuring the permeability of Eleana argillite from area 17, Nevada test site, using the transient method, *Rep. UCRL-52604*, 11 pp., Lawrence Livermore Natl. Lab., Livermore, Calif.
- Longstaffe, F. J., B. J. Tilley, A. Ayalon, and C. A. Connolly (1992), Controls on porewater evolution during sandstone diagenesis, western Canada sedimentary basin: An oxygen isotope perspective, in *Origin, Diagenesis, and Petrophysics of Clay Minerals in Sandstones*, edited by D. W. Houseknecht and E. D. Pittman, *Spec. Publ. SEPM Soc. Sediment. Geol.*, **47**, 13–34.
- Madsen, F. T., and M. Muller-Vonmoos (1985), Swelling pressure calculated from mineralogical properties of a Jurassic Opalinum shale, Switzerland, *Clays Clay Miner.*, **33**, 501–509.
- Magara, K. (1971), Permeability considerations in generation of abnormal pressures, *Soc. Pet. Eng. J.*, **11**, 236–242.
- Magara, K. (1974), Compaction, ion filtration, and osmosis in shale and their significance in primary migration, *AAPG Bull.*, **58**, 283–290.
- Magara, K. (1975a), Reevaluation of montmorillonite dehydration as cause of abnormal pressure and hydrocarbon migration, *AAPG Bull.*, **59**, 292–302.
- Magara, K. (1975b), Importance of aquathermal pressuring effect in Gulf Coast, *AAPG Bull.*, **59**, 2037–2045.
- McBride, M. B. (1989), Surface chemistry of soil minerals, in *Minerals in Soil Environments*, 2nd ed., edited by J. B. Dixon and S. B. Weed, pp. 35–88, Soil Sci. Soc. of Am., Madison, Wis.
- Meissner, F. F. (1978), Petroleum geology of the Bakken Formation, Williston Basin, North Dakota and Montana, paper presented at the 1978 Williston Basin Symposium, Mont. Geol. Soc., Billings.
- Mesri, G., and R. E. Olson (1971), Mechanisms controlling the permeability of clays, *Clays Clay Miner.*, **19**, 151–158.
- Meyer, C. A., R. B. McClintock, G. J. Silvestri, and R. C. Spence Jr. (1979), *ASME Steam Table, Thermodynamic and Transport Properties of Steam*, 330 pp., Am. Soc. of Mech. Eng., New York.
- Momper, J. A. (1978), Oil migration limitations suggested by geological and geochemical considerations, *AAPG Cont. Educ. Course Note Ser.* **8**, pp. B1–B55, Am. Assoc. of Pet. Eng., Tulsa, Okla.
- Moore, D. E., C. A. Morrow, and J. D. Byerlee (1982), Use of swelling clays to reduce permeability and its potential application to nuclear waste repository sealing, *Geophys. Res. Lett.*, **9**, 1009–1012.
- Morse, J. W., and F. T. Mackenzie (1990), *Geochemistry of Sedimentary Carbonates*, 707 pp., Elsevier Sci., New York.
- Morton, R. A., and L. S. Land (1987), Regional variations in formation water chemistry, Frio Formation (Oligocene), Texas Gulf Coast, *AAPG Bull.*, **71**, 191–206.
- Mungan, N. (1965), Permeability reduction through changes in pH and salinity, *J. Pet. Technol.*, **17**, 1449–1453.
- Mungan, N. (1968), Permeability reduction due to salinity changes, *J. Can. Pet. Technol.*, **7**, 113–117.
- Norrish, K. (1973), Factors in the weathering of mica to vermiculite, paper presented at the 1972 Proceedings on International Clay Conference.
- Olsen, H. W. (1972), Liquid movement through kaolinite under hydraulic, electric, and osmotic gradients, *Am. Assoc. Pet. Geol. Bull.*, **56**, 2022–2028.
- Pashley, R. M., and J. N. Israelachvili (1984), Molecular layering of water in thin films between mica surfaces and its relation to hydration forces, *J. Colloid Interface Sci.*, **101**, 511–523.
- Powers, M. C. (1967), Fluid-release mechanisms in compacting marine mudrocks and their importance in oil exploration, *Am. Assoc. Pet. Geol. Bull.*, **51**, 1240–1254.
- Revil, A., and L. M. Cathles III (1999), Permeability of shaly sands, *Water Resour. Res.*, **35**, 651–662.
- Revil, A., and P. Leroy (2004), Constitutive equations for ionic transport in porous shales, *J. Geophys. Res.*, **109**, B03208, doi:10.1029/2003JB002755.
- Schlomer, S., and B. M. Krooss (1997), Experimental characterization of the hydrocarbon sealing efficiency of cap rocks, *Mar. Pet. Geol.*, **14**, 565–580.
- Schmidt, G. W. (1973), Interstitial water composition and geochemistry of deep Gulf Coast shales and sandstones, *Am. Assoc. Pet. Geol. Bull.*, **57**, 321–337.
- Scott, A. D., and S. J. Smith (1966), Susceptibility of interlayer potassium in micas to exchange with sodium, *Clays Clay Miner.*, **14**, 69–81.
- Sharp, J. M., Jr. (1983), Permeability controls on aquathermal pressuring, *AAPG Bull.*, **67**, 2057–2061.
- Siever, R., K. C. Beck, and R. A. Berner (1965), Composition of interstitial waters of modern sediments, *J. Geol.*, **73**, 39–73.
- Singh, U., and G. Uehara (1986), Electrochemistry of the double-layer: Principles and applications to soils, in *Soil Physical Chemistry*, edited by D. L. Sparks, pp. 1–38, CRC Press, Boca Raton, Fla.
- Smith, R. E., and D. V. Wiltschko (1996), Generation and maintenance of abnormal fluid pressures beneath a ramping thrust sheet: Isotropic permeability experiments, *J. Struct. Geol.*, **18**, 951–970.
- Sparks, D. L. (1995), *Environmental Soil Chemistry*, 267 pp. Academic, San Diego, Calif.
- Spencer, C. W. (1987), Hydrocarbon generation as a mechanism for overpressuring in Rocky Mountain region, *AAPG Bull.*, **71**, 368–388.
- Spencer, C. W. (1994), Abnormal formation pressures caused by hydrocarbon generation: Examples from the Rocky Mountain region, in *Studies in Abnormal Pressures*, edited by W. H. Fertl, R. E. Champman, and R. F. Hotz, pp. 343–375, Elsevier Sci., New York.
- Sposito, G. (1984), *The Surface Chemistry of Soils*, 234 pp., Oxford Univ. Press, New York.
- Sposito, G., N. T. Skipper, R. Sutton, S.-H. Park, A. K. Soper, and J. A. Greathouse (1999), Surface geochemistry of the clay minerals, *Proc. Natl. Acad. Sci.*, **96**, 3358–3364.
- Steiger, R. P. (1993), Advanced triaxial swelling tests on preserved shale cores, *Int. J. Rock Mech. Min. Sci.*, **30**, 681–685.
- Sutherland, H. J., and S. P. Cave (1980), Argon gas permeability of New Mexico rock salt under hydrostatic compression, *Int. J. Rock Mech. Min. Sci.*, **17**, 281–288.
- Timm, B. C., and J. J. Maricelli (1953), Formation waters in southwest Louisiana, *Am. Assoc. Pet. Geol. Bull.*, **37**, 394–409.

- Trimmer, D. A. (1981), Design criteria for laboratory measurements of low permeability rocks, *Geophys. Res. Lett.*, *8*, 973–975.
- Van Olphen, H. (1977), *An Introduction to Clay Colloid Chemistry*, 2nd ed., 318 pp., John Wiley, Hoboken, N. J.
- Van Olphen, H., and J. J. Fripiat (1979), *Data Handbook for Clay Materials and Other Non-metallic Minerals*, 346 pp., Pergamon, New York.
- Vavra, C. L., J. G. Kaldi, and R. M. Sneider (1992), Geological applications of capillary pressure: A review, *AAPG Bull.*, *76*, 840–850.
- Weinbrandt, R. M., and I. Fatt (1970), Scanning electron microscope study of the pore structure of sandstone, *Proc. U.S. Symp. Rock Mech.*, *11th*, 629–641.
- Whitworth, T. M., and S. J. Fritz (1994), Electrolyte-induced solute permeability effects in compacted smectite membranes, *Appl. Geochem.*, *9*, 533–546.
- Wolf, A. V., M. G. Brown, and P. G. Prentiss (1979), Concentrative properties of aqueous solutions: Conversion tables, in *CRC Handbook of Chemistry and Physics*, 60th ed., edited by R. C. Weast, pp. D227–D276, CRC Press, Boca Raton, Fla.
- Young, A., P. F. Low, and A. S. McLatchie (1964), Permeability studies of argillaceous rocks, *J. Geophys. Res.*, *69*, 4237–4245.

B. E. Herbert and A. K. Kronenberg, Department of Geology and Geophysics, Texas A&M University, College Station, TX 77843, USA. (kronenberg@geo.tamu.edu)

O. Kwon, Core Laboratories, Petroleum Services, 6316 Windfern, Houston, TX 77040, USA.